Measurements of the Complete Solvation Response in Ionic Liquids †

4 AUTHORS, INCLUDING:

Gary A Baker
University of Missouri

246 PUBLICATIONS **8,820** CITATIONS

Mark Maroncelli
Pennsylvania State University

126 PUBLICATIONS **11,752** CITATIONS

Measurements of the Complete Solvation Response in Ionic Liquids[†]

Sergei Arzhantsev,[‡] Hui Jin,[‡] Gary A. Baker,[§] and Mark Maroncelli*,[‡]

Department of Chemistry, The Pennsylvania State University, 104 Chemistry Building,
University Park, Pennsylvania 16802, and Chemical Sciences Division, Oak Ridge National Laboratory,
P.O. Box 2008, Oak Ridge, Tennessee 37831-6110

Received: November 4, 2006; In Final Form: January 2, 2007

Dynamic Stokes shift measurements of the solvatochromic probe *trans*-4-dimethylamino-4′-cyanostilbene were used to measure the solvation response of five imidazolium and one pyrrolidinium ionic liquid at 25 °C. The Kerr-gated emission and time-correlated single-photon-counting techniques were used to measure spectral dynamics occurring over the time ranges of 100 fs–200 ps and 50 ps–5 ns, respectively, and a combination of data sets from these two techniques enabled observation of the complete solvation response. Observed response functions were found to be biphasic, consisting of a sub-picosecond component of modest (10–20%) amplitude and a dominant slower component relaxing over times of a few picoseconds to several nanoseconds. The faster component could be correlated to inertial characteristics of the constituent ions, and the slower component to solvent viscosity. Dielectric continuum calculations of the sort previously used to predict solvation dynamics in dipolar liquids were shown to work poorly for predicting the response in these ionic liquids.

1. Introduction

Widespread interest in the potential use of room-temperature ionic liquids as solvents in a variety of contexts has engendered study of the nature of solvation in these distinctive media.[1,2] In addition to many reports addressing the equilibrium "polarity" and solvating abilities of ionic liquids,[2–5] a number of recent papers have explored dynamical aspects of solvation in these solvents. Such studies include measurements of ultrafast polarizability dynamics[6–14] and dielectric dispersion in neat ionic liquids[15–20] as well as studies concerned with the time-dependent response to solute-induced perturbations.[19–47] The latter dynamics, especially the response of a solvent to an electrical perturbation of a solute, commonly known as "polar solvation dynamics",[21] is the topic of the present paper. Characterizing such dynamics is of interest both for the new perspectives it provides on fundamental aspects of liquid-phase dynamics and also for its relevance to understanding how ultrafast chemical reactions, especially charge-transfer processes, couple to an ionic-liquid environment.

Measurements of polar solvation dynamics in ionic liquids actually began with the work of Huppert and co-workers,[22–25] prior to all of the recent interest in these solvents. These authors measured Stokes shift dynamics of several probe solutes in a number of tetraalkyammonium fused salts whose melting points (105–170 °C) place them on the border of what would now be considered "room-temperature" ionic liquids. The first measurements on modern ionic liquids, based on the imidazolium cation, were made by Karmakar and Samanta in 2002.[26,27] Subsequent work by Samanta and co-workers[28–31] as well as contributions by our group[32–37] and those of Sarkar,[38–42] Petrich,[43–46] Richert,[19,20] and others[47–49] have resulted in the accumulation

of a sizable database on solvation dynamics in ionic liquids. Samanta has recently reviewed much of this work[50,51] so that here we will only highlight some of the emerging trends.

Nearly all measurements to date have employed time-correlated single-photon-counting (TCSPC) or other time-resolved emission techniques having time resolutions in the 25–100 ps range. Although there can be considerable variability in the quantitative results reported by different groups for the same ionic liquid[35,43] (especially in the case of highly viscous liquids[50]) the general features are consistent in all cases. In picosecond experiments the solvation energy is observed to relax in a nonexponential manner, typically over times of tens of picoseconds to several nanoseconds. Some authors chose to fit this relaxation using biexponential functions of time and interpret these times in terms of two distinct types of solvent motion[26–31] whereas we[32–34] and others[19,20,35] prefer to employ a stretched-exponential representation and view the nonexponential relaxation as resulting from a single but complex dynamical process that resembles the dynamics occurring in supercooled liquids. Independent of how one chooses to fit the data, a clear correlation exists between the integral solvation times measured in such experiments and solvent viscosity. This relationship to viscosity is obvious in measurements performed in a single ionic liquid as a function of temperature,[19,20,32,33,35] but it is also often found that approximately the same relationship between solvation times and viscosity holds across a number of different ionic liquids.[31,33,34,36,44] A variety of probe solutes have been employed to measure solvation dynamics, the most popular among these being coumarin 153 (C153). When measurements are conducted in a single laboratory it is generally found that different probes yield comparable solvation times,[50,51] but in a few cases variations of factors of 2–3 have been reported.[31,35]

Despite the fact that integral solvation times observed in the aforementioned experiments are often in the nanosecond range, it was recognized early on that a substantial portion of the solvent relaxation is often missed.[32] In many ionic liquids,
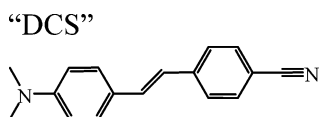
Complete Solvation Response in Ionic Liquids

J. Phys. Chem. B, Vol. 111, No. 18, 2007 **4979**

SCHEME 1

"DCS"

steady-state estimates of the expected time-zero spectrum[52] have indicated that roughly half of the solvation response is too rapid to be observed in experiments with 25 ps or longer instrumental response times.[31-33,35,44] This observation appeared to be consistent with the prediction of substantial (often >50%) sub-picosecond components in simulations of model systems[53-61] described later in section 3E.

To date there have been very few experiments performed with the time resolution necessary to observe such a fast component of the response. In the first attempt, Petrich and co-workers[43] used stimulated emission of C153 measured with sub-picosecond resolution at certain special wavelengths[62] to estimate the solvation response in several imidazolium ionic liquids. Unfortunately, the results were ambiguous in that the fastest time constants observed (40-70 ps) were clearly inconsistent with the authors' own preliminary fluorescence upconversion data, which suggested times on the order of 7 ps.[43] Very recently, Lang et al.[49] reported fluorescence upconversion measurements (230 fs instrument response) of C153 in two imidazolium ionic liquids. Using triple-exponential fits, these authors reported only modest (8-16%) relaxation on the sub-picosecond time scale (0.6 and 0.9 ps) with the bulk of the dynamics taking place with time constants of greater than 25 ps. Such a small contribution from sub-picosecond components appears to be at odds with most simulation results as well as with estimates based on TCSPC measurements and time-zero estimates. However, these results must be viewed with caution. The fact that the Stokes shift magnitudes reported by Lang et al.[49] are less than half of those measured for C153 in comparable ionic liquids but with much lower time resolution[35,43,44] suggests that some sort of artifact severely distorts their data. Finally, our group has reported preliminary studies that combine spectra from Kerr-gated emission (KGE; 450 fs response)[63] and TCSPC (25 ps response) experiments to monitor solvation dynamics in three imidazolium ionic liquids.[37] In that work we found that the solvation components not observed with TCSPC were not all contained in a large sub-picosecond component as had been originally anticipated. Instead, as did Lang et al.,[49] we found that only a small (10-20%) distinct sub-picosecond component was required to fit the data. The remaining components missed in TCSPC experiments were attributed to the fastest parts of the single broadly distributed process observed to comprise the second phase of the relaxation.

The present report describes a more complete series of combined KGE + TCSPC measurements designed to observe the full solvation response in ionic liquids. Here we present results obtained using the solvation probe *trans*-4-dimethylamino-4′-cyanostilbene (Scheme 1; DCS) to measure solvation dynamics in the five imidazolium and one pyrrolidinium ionic liquids shown in Table 1. After describing our experimental methods, the results of this work are presented in six sections. We first (section 3A) make comparisons between DCS and the more widely used solvation probe C153 to demonstrate that these two probes provide equivalent dynamical information in ionic liquids. In section 3B we present the main results of KGE + TCSPC experiments. As in our previous work,[37] we find that the solvation response in ionic liquids is biphasic, consisting of both a rapid sub-picosecond component and a much longer component relaxing over picosecond and nanosecond times. We

show that the amplitude and time constant of the fast component can be correlated to inertial characteristics of the ions involved whereas the longer component is related to solvent viscosity. In section 3C we briefly consider what the present measurements imply about the accuracy of results obtained from TCSPC and other measurements with comparable time resolutions. We find that despite distortions of the early time data integral solvation times measured from such experiments can still provide a useful characterization of the second component of the response in ionic liquids. Comparisons between the observed solvation response and the simple dielectric continuum calculations are then carried out for three ionic liquids in section 3D. We find that the same relationships that accurately connect dielectric and solvation data in conventional dipolar liquids are of little value for predicting solvation dynamics in ionic liquids. In section 3E we compare our experimental results to available computer simulations of solvation dynamics in ionic liquids, and find that there is general agreement concerning to the inertial component of the response. Finally, in section 3F we conjecture about the molecular mechanisms of solvation in these systems.
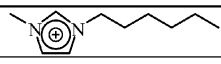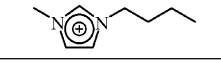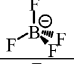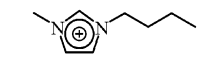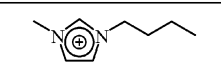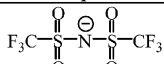
2. Experimental Methods

trans-4-Dimethylamino-4′-cyanostilbene was obtained from Klaas Zachariasse and used as received. Electrochemical-grade 1-butyl-3-methylimidazolium hexafluorophosphate [Im$_{41}^+$][PF$_6^-$], *bis*-(trifluoromethylsulfonyl)imide [Im$_{41}^+$][Tf$_2$N$^-$], and *tris*(trifluoromethylsulfonyl)methide [Im$_{41}^+$][Tf$_3$C$^-$] were purchased from Covalent Associates and were also used as received. 1-Butyl-3-methylimidazolium tetrafluoroborate [Im$_{41}^+$][BF$_4^-$] was purchased from Aldrich (97%) and purified by dissolving it in acetonitrile, treating it with activated carbon for 12 h, running the solution through a neutral activated alumina column, and evaporating the solvent in a rotary evaporator. The [Im$_{41}^+$][BF$_4^-$] was then dried by heating to approximately 60 °C under vacuum for 36 h. *n*-Propyl-*n*-methylpyrrolidinium *bis*-(trifluoromethylsulfonyl)imide [Pr$_{31}^+$][Tf$_2$N$^-$] was prepared according to published methods.[64] The synthesis of 1-hexyl-3-methylimidazolium chloride [Im$_{61}^+$][Cl$^-$] was adapted from methods described by Nockemann et al.,[65] with some essential variations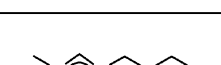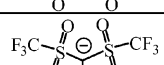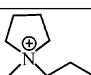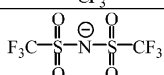. These latter two ionic liquids were dried under vacuum at 70 °C for 48 h and characterized by ^{1}H NMR spectroscopy. Full details on our routes to these and other spectrochemical-grade ionic liquids will be reported elsewhere.[66] All ionic liquids were stored in a nitrogen-purged glove box where samples were made up in vials and then transferred to 1 cm sealed quartz cuvettes for steady-state and TCSPC measurements. Samples for KGE measurements were contained in a recirculating flow system during measurements. This flow system was sealed from contact with the atmosphere to reduce the potential for uptake of moisture. After running the KGE experiments the water contents of the samples were checked by coulometric Karl Fischer titration (Mettler-Toledo DL32). The weight percentage of water was generally found to be approximately 400 ppm, with the exception of [Im$_{61}^+$][Cl$^-$] where the water content was 2% by weight.

All experiments reported here were carried out at 25 °C. The temperatures of the static samples used for steady-state and TCSPC experiments were controlled to within 0.1 °C using circulating water baths. Temperature control of ±0.5 °C was achieved in the flow system of the KGE experiments by surrounding the tubing, pump head, and sample vial with flexible heaters.

Steady-state absorption spectra were measured using a Hitachi U-3010 UV/vis spectrophotometer, and corrected emission spectra with a Spex Fluorolog F212 fluorimeter. Picosecond

TABLE 1: Ionic Liquids Studied

#	Liquid	Cation	R_+ / Å	m_+ / m_u	Anion	R_- / Å	m_- / m_u	η / cP
1	$[Im_{61}^+][Cl^-]$		3.57	167	Cl^-	2.09	35	660
2	$[Im_{41}^+][BF_4^-]$		3.39	139		2.29	87	75
3	$[Im_{41}^+][PF_6^-]$		3.39	139		2.72	145	190
4	$[Im_{41}^+][Tf_2N^-]$		3.39	139		3.39	280	42
5	$[Im_{41}^+][Tf_3C^-]$		3.39	139		3.81	411	260
6	$[Pr_{31}^+][Tf_2N^-]$		3.47	128		3.39	280	53

R_+ and R_- are cation and anion radii derived from van der Waals volumes $R = (3V_{vdW}/4\pi)^{1/3}$. The latter are electronic volumes from B3LYP/6-31G(d,p) calculations[98] adjusted to best reproduce van der Waals increments of Bondi.[99] M_+ and M_- are ion masses, and η is the viscosity at 25 °C.[98]

time-resolved emission measurements were made using a time-correlated single-photon-counting system based on 390 nm excitation from the doubled output of a femtosecond Ti:sapphire laser.[67] The overall response time of this system was 25 ps (full width at half-maximum) as measured by a scattering solution. A series of up to 16 magic angle decays recorded at wavelengths spanning the emission spectrum were collected through a monochromator with a bandpass of 8 nm. After partially removing the effect of instrumental broadening by iterative reconvolution fitting, the fitted decays were used to reconstruct time-resolved emission spectra as described in ref 68.

Femtosecond time-resolved emission measurements were made using a home-built spectrometer based on optical Kerr gating, which is described in detail in ref 63. Briefly, a 250 kHz amplified Ti:sapphire laser system (Coherent, Rega 9050) is used as the light source. The output of this laser system is split into two beams with intensities in a ratio of 1:3. The smaller portion is doubled in a β-barium borate (BBO) crystal and used to excite the sample while the larger portion is used for the Kerr gate. The exciting light (387 nm) is focused into a 1 mm quartz flow cell containing the sample. The optical densities of the samples used were between 1 and 3 to minimize the effect of Raman scattering from the solvents. Fluorescence from the sample is collected by an off-axis parabolic mirror and focused by a lens into the 1 mm static Kerr cell containing liquid benzene placed between a pair of crossed polarizers. Gated emission is dispersed in a spectrograph (Acton, SpectraPro-300i) and detected by a liquid-nitrogen-cooled CCD camera (Princeton Instruments). Data were collected under magic angle conditions by rotating the excitation polarization using a half wave plate. The instrument response, estimated as the full width at half-maximum of the Raman scattering signal from cyclohexane, was approximately 450 fs, and the spectral resolution was approximately 3−4 nm in these experiments.

Most of the dynamics observed here are adequately captured by the 450 fs instrumental response of the KGE experiment. However, to ensure that some of the fast dynamics were not missed due to the finite instrument response, iterative reconvolution fitting was performed. Details of the fitting procedures are provided in ref 63. Spectral data covering 1.2 nm intervals over the range of 395−625 nm were first averaged to produce a reduced data set consisting of approximately 200 temporal decays. These decays were then simultaneously fit to sums of 5 or 6 exponential functions with fixed time constants, using the Raman scattering signal from cyclohexane as the instrumental response function. The time-resolved spectra were constructed from the fitted decays and then corrected for spectral sensitivity.

Two levels of spectral correction were necessary in the KGE experiments. A coarse correction, based on the system response to several dye solutions,[69] was first applied to the data. For typical solvents having dynamics of a few picoseconds, such a correction typically provides spectra at long times that are within 150 cm^{-1} (4 nm) of the steady-state spectra. To achieve better agreement, a second level of correction is required. For these slowly relaxing liquids, we used comparisons of the KGE data to log-normal fits of the TCSPC data between 20 and 100 ps to provide this second level of correction. Such corrections do not significantly alter the time dependence of the spectral frequencies reported. The effect is primarily one of shifting the frequencies of the spectra by a small fraction of their width, which allows for a smoother splice between the KGE and the TCSPC data. Finally, although most samples employed here had optical densities close to unity, in some cases much higher OD samples were used. In these cases an additional spectral correction, based on the sample absorption, had to be applied to account for reabsorption of the blue edge of the emission spectrum.

3. Results and Discussion

A. DCS as a Solvation Probe. Before describing the results of the KGE + TCSPC measurements, we first briefly consider the use of DCS as a solvation probe in ionic liquids. The solvatochromic behavior of DCS in conventional solvents has been previously characterized in a number of studies.[70−72] Although DCS is flexible and it undergoes the photoisomerization common to most stilbenes,[73,74] in a recent paper we proposed DCS as a simple probe of both equilibrium and nonequilibrium solvation, comparable in most respects to the best-known probe C153.[68] In that study we found the solvation

Complete Solvation Response in Ionic Liquids

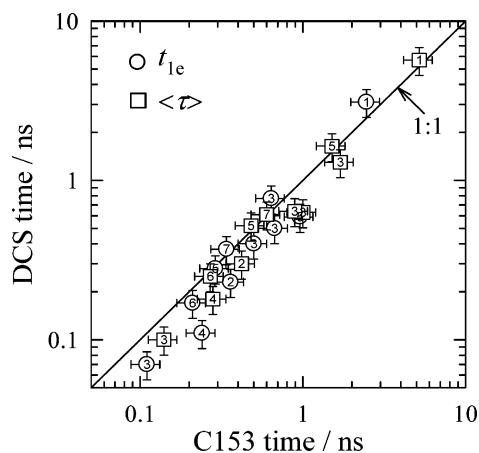*J. Phys. Chem. B, Vol. 111, No. 18, 2007* **4981**

Figure 1. Comparison of $1/e$ (circles) and integral (squares) times of the spectral shift dynamics observed in C153 and DCS using TCSPC. Numbers here refer to different ionic liquids as listed in Table 1. The no. 7 denotes the additional liquid $[N(n\text{-}C_4H_9)(iso\text{-}C_3H_7)(CH_3)_2^+]$-$[Tf_2N^-]$.

response measured with DCS in a range of polar aprotic solvents to be within experimental uncertainties of that measured using C153.[71] In protic solvents, however, the solvation times measured with DCS were systematically faster (by approximately a factor of 2) than those measured with C153, for reasons that are not yet clear. In another study, we compared the dynamic Stokes shifts of DCS and C153 along with several other solutes in $[Im_{41}^+][PF_6^-]$ using the TCSPC technique.[35] Comparisons were hampered by the fact that roughly half of the solvation response was too fast to be observed in these experiments. Nevertheless, significant ($\sim$2-fold) variations were found in the solvation times reported by different solutes, and DCS was observed to be the fastest among the six solutes examined. One might therefore question whether DCS measures the same nonspecific solvation dynamics in ionic liquids that one expects from a more standard probe such as C153.

To address this question we have measured the dynamics of both DCS and C153 in seven different ionic liquids using the TCSPC technique. The results are summarized in Figure 1. Here we focus only on the portion of the spectral dynamics observable with the 25 ps response function of our TCSPC instrument and compare $1/e$ and integral ($\langle\tau\rangle$) times of the observed spectral shifts. As illustrated in Figure 1, the times measured with these two solutes nearly agree to within their combined uncertainties ($\pm20\%$), but there is a modest systematic bias such that the times measured with DCS are on average 22% smaller than those measured with C153. This difference may indicate a real distinction between the dynamics sensed by these two probes, but it seems more likely that it merely reflects the influence of the nearly 2-fold larger Stokes shifts of DCS ($\sim$4000 cm^{-1}) relative to those of C153 ($\sim$2000 cm^{-1}). It is expected that larger spectral shifts facilitate the detection of faster components of the dynamics and thus lead to smaller observed times in DCS compared to those of C153. Either way, the small differences between these two probes serve to validate the use of DCS to monitor nonspecific solvation dynamics in ionic liquids.

B. Results of KGE + TCSPC Measurements. Figure 2 shows a representative set of KGE + TCSPC spectral data of DCS in $[Im_{41}^+][PF_6^-]$. The spectra at times less than 100 ps are from the KGE experiment and are shown after reconvolution fitting and spectral correction. These spectra are essentially continuous functions of frequency. Later-time spectra are from TCSPC data recorded at a series of 16 frequencies (points).
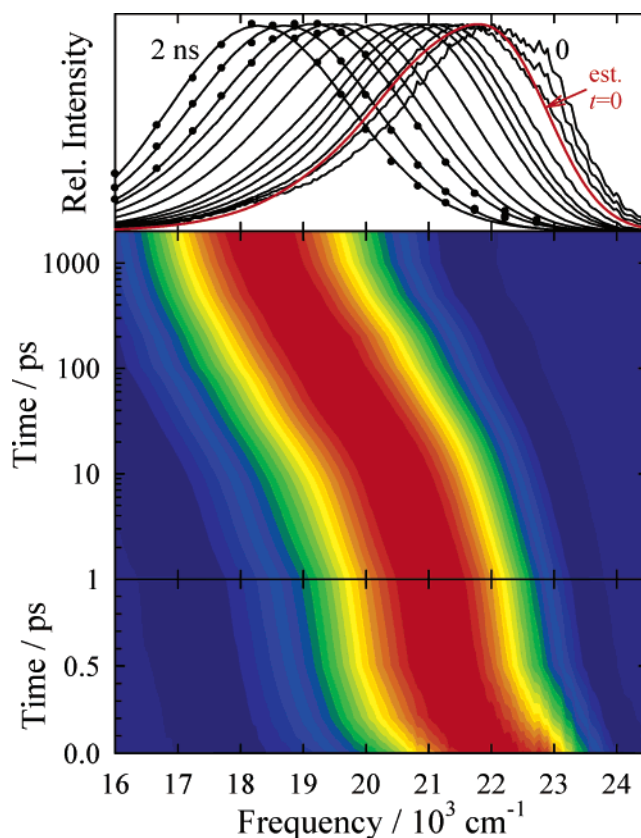

Figure 2. Time-resolved emission spectra of DCS in $[Im_{41}^+][BF_4^-]$. The colored panels are a continuous representation of the spectral data in the form of a contour plot. The top panel shows a series of spectra at times of 0, 0.1, 0.2, 0.5, 1, 2, 5, 20, 50, and 100 ps using the KGE technique and at 0.2, 0.5, and 2 ns using the TCSPC technique. In the latter case data were collected at the set of 16 discrete frequencies indicated by the points and then fit to log-normal line shape functions indicated by the smooth curves through these points. The red curve labeled "est. $t = 0$" is the estimated time-zero spectrum (see text). All spectra have been normalized to the same peak height. (The emission lifetime of DCS in $[Im_{41}^+][BF_4^-]$ is $\sim$1.4 ns, and the spectral intensity actually decreases by $\sim$75% over the 2 ns time window shown.)

These data are fit to log-normal line shape functions to obtain a continuous representation. In general, we do not observe any noteworthy changes in the spectral width or shape with time. The widths of both steady-state and time-resolved spectra of DCS in ionic liquids lie in the range 3400 ± 200 cm^{-1}. What variations we do observe tend to fall within the uncertainties of the experimental data, whose accuracy is limited by Raman scattering at early times ($\sim$22 800 cm^{-1} in Figure 2) and solvent emission at times long in comparison to the DCS lifetime (1.2–1.8). We therefore hereafter focus on the time evolution of the peak frequencies $\nu_p(t)$ of spectra such as these, which are determined most reliably.

Figure 3 provides three examples of peak frequency data $\nu_p(t)$ that we use to characterize the solvation response. These $\nu_p(t)$ data are biphasic, consisting of a short-time component in the $\sim$1 ps time range and then longer components in the 10 ps–10 ns time range. In all cases studied such data can be fit to within uncertainties by a function of the form

$$\nu_p(t) = \nu_p(\infty) + \Delta\nu_p\{f_1 \exp(-t/\tau_1) +$$
$$(1 - f_1) \exp[-(t/\tau_2)^\beta]\} \quad (1)$$

The smooth curves in Figure 3 are fits of the experimental data (circles) to this function. The dashed lines indicate the contribu-
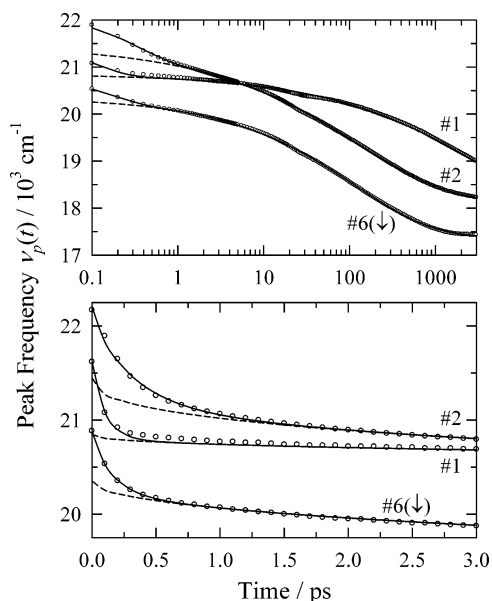
Figure 3. Time evolution of the peak frequencies of DCS in three ionic liquids, $1 = [\text{Im}_{61}^+][\text{Cl}^-]$, $2 = [\text{Im}_{41}^+][\text{BF}_4^-]$, and $6 = [\text{Pr}_{31}^+][\text{Tf}_2\text{N}^-]$. Points denote experimental data, solid curves are fits of these data to eq 1, and dashed curves show only the stretched-exponential components of these fits. As indicated by the arrows, the frequencies of the no. 6 data have been shifted downward by 1000 cm^{-1} to remove overlap with the remaining data. Note that the slightly discontinuous slopes in the experimental data near 30 ps indicate where KGE and TCSPC data are spliced together.

tion of the dominant second component, which we take to have a stretched-exponential time dependence. Deviations at early times indicate the need for an additional fast component, which is most simply represented using an exponential time dependence.[75]

Parametrizations of the experimental data according to eq 1 are provided in Table 2. Also listed in the last columns of this table are estimates of the expected magnitude of $\Delta\nu_p$ based on estimates of the position of the spectrum prior to solvent relaxation. An example of an estimated "time-zero" spectrum used for these evaluations is provided in the top panel of Figure 2. Such spectra are obtained via the method described in ref 71, which differs slightly from our usual approach[52] to better account for changes in the vibronic structure of the DCS emission with solvent polarity. (For this reason, some of the estimated values of $\Delta\nu_p$ listed here differ by up to 250 cm^{-1} from earlier values.[37]) Note that in Figure 2 the peak of the spectrum measured at the earliest time lies at a higher frequency of the peak of this estimated spectrum, by approximately 400 cm^{-1}. As indicated in the final column of Table 2, such a displacement means that in this worst case the observed and predicted Stokes shift magnitudes differ by 12%. In other cases the estimated and observed values of $\Delta\nu_p$ differ by an average of <4% (140 cm^{-1}). We consider these differences to be within the combined uncertainties of the KGE data and the estimated time-zero spectra and therefore assume in what follows that we have in all cases observed the entire spectral dynamics. Thus, we consider the true spectral or solvation response function $S_\nu(t)$ to be given by these fits according to

$$S_\nu(t) = \frac{\nu_p(t) - \nu_p(\infty)}{\nu_p(0) - \nu_p(\infty)} \cong f_1 \exp(-t/\tau_1) + \qquad (1 - f_1) \exp[-(t/\tau_2)^\beta] \quad (2)$$

Characteristics of the faster component of the response are examined in Figure 4. As will be discussed in detail in section

3E, this component of the response can be equated to the sub-picosecond Gaussian component reported in several simulation studies.[53–61] Such simulations indicate that the motion involved in this fast component is primarily inertial translation of ions; however it is not yet clear how one might simply model these motions. In Figure 4 we attempt to correlate the amplitude f_1 and time constant τ_1 of the fast component of the response with the product $\sqrt{\mu_\pm(R_+ + R_-)^3}$ where $\mu_\pm$ is the reduced mass of an ion pair and $(R_+ + R_-)$ is the sum of their van der Waals radii (Table 1). Use of this particular quantity is motivated by the fact that the vibrational frequency of an ion pair calculated assuming a spherical pair potential consisting of a short-range repulsion and an electrostatic attraction[76] is proportional to $1/\sqrt{\mu_\pm \Delta R_{eq}^3}$ where ΔR_{eq} is the equilibrium pair separation. We note that Debye frequencies of alkali halide crystals are well represented ($N = 13$, $r^2 = 0.97$) by a simple proportionality to this factor. As shown in Figure 4 there is a reasonable correlation of both f_1 and τ_1 with this factor, especially if the non-imidazolium liquid (no. 6) is excluded. Other quantities such as $\mu_\pm^{1/2}$ (but not m_- alone) provide correlations of comparable quality to those shown in Figure 4. Our choice of the factor $\sqrt{\mu_\pm(R_+ + R_-)^3}$ is not intended to imply any particular mechanism; it is merely used to empirically demonstrate the connection between the fast component and inertial motion.

The slow portion of the dynamics is well represented by a stretched-exponential function of time. The shapes of this portion of the response, as indicated by the values of β in Table 2, are similar in all cases except $[\text{Im}_{41}^+][\text{PF}_6^-]$. We illustrate this similarity in Figure 5 by plotting normalized slow-component response functions

$$S_2(t) = \{S(t) - f_1 \exp(-t/\tau_1)\}/(1 - f_1) \cong \exp[-(t/\tau_2)^\beta] \quad (3)$$

versus time reduced by τ_2. In all cases, the relaxation of $S_2(t)$ is distributed over 3–4 decades in time. The distinction between these dynamics and a simple exponential relaxation is emphasized by comparison to the exponential function ($\beta = 1$) shown in Figure 5. To within anticipated uncertainties the various functions are all the same except for the $[\text{Im}_{41}^+][\text{PF}_6^-]$ case. Why $[\text{Im}_{41}^+][\text{PF}_6^-]$ should differ from the other liquids is not clear. We note, however, that Ito and Richert[20] recently reported very similar relaxation dynamics measured with a phosphorescent probe in $[\text{Im}_{41}^+][\text{PF}_6^-]$ near its glass transition (194 K). These authors were able to fit time–temperature data recorded over 6 decades in t/τ_2 to a stretched-exponential function with a value of $\beta = 0.30 \pm 0.03$. Interestingly, the one other ionic liquid on which these authors made comparable measurements yielded a stretched-exponential relaxation with $\beta = 0.40 \pm 0.05$, which is similar to what we observe in the other liquids.[19]

Figure 6 illustrates the fact that the times associated with the slower component of the dynamics, both τ_2 and the integral time $\langle\tau\rangle = \int_0^\infty S_2(t) \, dt = \tau_2\Gamma(\beta^{-1})/\beta$, scale approximately with the bulk solvent viscosity. The fits shown here are not directly proportional to viscosity η but rather to η^p where $p \approx 1.2–1.3$. Results from previous experiments with lower time resolution (where much of the relaxation is too fast to be observed) have already pointed out this relationship to viscosity.[30,32–34,36,37,44] It appears to provide good correlations of the data collected in a single ionic liquid at different temperatures[32,33] or in a series of ionic liquids whose cations do not vary greatly in size[30,34,36,37,44] as is the case here. Such scaling with viscosity suggests coupling to structural reorganization in the solvent, as will be discussed later.

Complete Solvation Response in Ionic Liquids

J. Phys. Chem. B, Vol. 111, No. 18, 2007 **4983**

TABLE 2: Fits Characterizing Peak Frequency Shifts $\nu_p(t)^a$

no.	liquid	ν_∞ (10^3 cm^{-1})	$\Delta\nu$ (10^3 cm^{-1})	f_1	τ_1 (ps)	τ_2 (ns)	β	$\langle\tau\rangle$ (ns)	$\Delta\nu_{est}$ (10^3 cm^{-1})	f_{obs}
1	[Im$_{61}^+$][Cl$^-$]	17.83	3.79	0.20	0.10	3.2	0.41	7.9	3.97	0.96
2	[Im$_{41}^+$][BF$_4^-$]	18.13	4.08	0.19	0.32	0.13	0.41	0.34	3.65	1.12
3	[Im$_{41}^+$][PF$_6^-$]	18.11	4.24	0.19	0.33	0.14	0.31	1.0	4.03	1.05
4	[Im$_{41}^+$][Tf$_2$N$^-$]	18.44	3.92	0.10	0.74	0.078	0.46	0.17	3.85	1.02
5	[Im$_{41}^+$][Tf$_3$C$^-$]	18.25	4.19	0.11	0.67	0.48	0.45	1.0	4.16	1.01
6	[Pr$_{31}^+$][Tf$_2$N$^-$]	18.39	3.50	0.15	0.15	0.12	0.48	0.21	3.85	0.91

^{a} ν_∞, $\Delta\nu$, f_1, τ_1, τ_2, and β are parameters of fits of the $\nu_p(t)$ data to eq 1. $\langle\tau\rangle$ is the integral relaxation time from the fit. $\Delta\nu_{est}$ is the magnitude of the solvation Stokes shift estimated from steady-state spectra as described in the text, and f_{obs} is $\Delta\nu/\Delta\nu_{est}$. Uncertainties are expected to be on the order of ±200 cm^{-1} for frequencies, $\pm16\%$ for f_1, $\pm25\%$ for τ_1, $\pm20\%$ for τ_2 and $\langle\tau\rangle$, and ±0.05 for β.
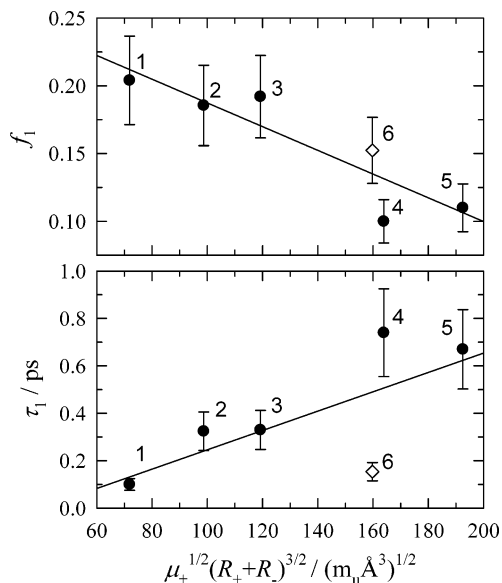

Figure 4. Correlation of the amplitude f_1 and time constant τ_1 associated with the fast solvation component with the inertial factor $\sqrt{\mu_\pm(R_+ + R_-)^3}$. The lines shown here are least-squares fits of all of the data. Correlation coefficients of these fits are $r^2 = 0.82$ (f_1) and 0.49 (τ_1). If the non-imidazolium liquid no. 6 is omitted from the fits the values of r^2 change to 0.86 (f_1) and 0.89 (τ_1).
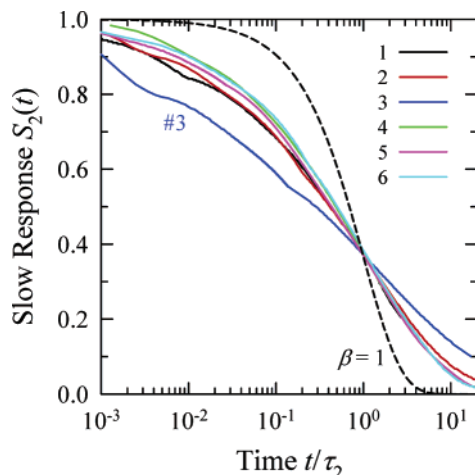

Figure 5. Scaled representations of the slower component of the dynamics $S_2(t)$ defined by eq 3. Times are scaled to the fitted stretched-exponential time τ_2. The dashed curve labeled "$\beta = 1$" is a single-exponential function for comparison.

C. Implications for TCSPC and Other Lower Resolution Methods. Because a considerable amount of data has already been collected with TCSPC and other methods that are not able to fully resolve the fastest portions of the solvation response, it is useful to consider what the present results imply about these
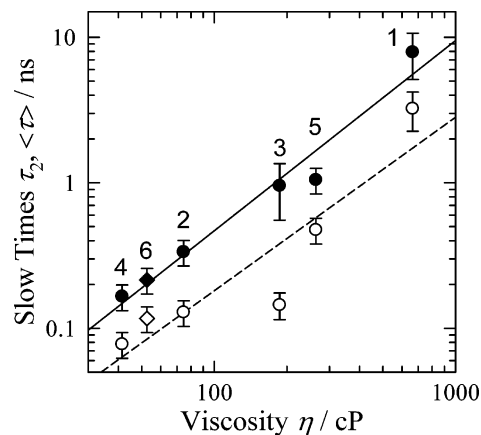

Figure 6. Times associated with the slow solvation component plotted against solvent viscosity. Open symbols are τ_2 times, and filled symbols are integral times $\langle\tau\rangle$ of the slow component. The least-squares lines shown here ($r^2 = 0.84$ for τ_2 and 0.96 for $\langle\tau\rangle$) imply times proportional to η^p with powers $p = 1.2$ for τ_2 and 1.3 for $\langle\tau\rangle$.
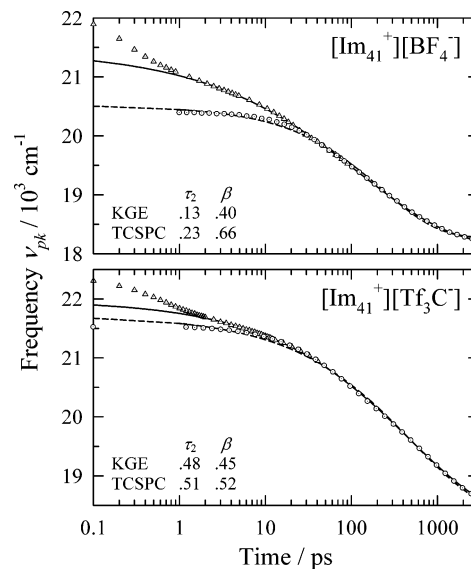
Figure 7. Comparison of fits of KGE + TCSPC data (triangles) neglecting the fast component of the response and TCSPC data alone (circles) in two ionic liquids. Stretched-exponential fits are shown as the solid (KGE + TCSPC) and dashed (TCSPC) curves, and the fit parameters are tabulated in the insets.

data. In particular, although such measurements inevitably miss the faster sub-picosecond portion of the dynamics, it is relevant to ask to what extent they can still be expected to accurately report on the slower portion of the dynamics. In Figure 7 we compare the $\nu_{pk}(t)$ dependence measured for DCS in two ionic liquids obtained (i) by combining KGE and TCSPC data and (ii) from the TCSPC data alone. Note that beyond times of 50–100 ps the same set of TCSPC data is used in constructing

4984 *J. Phys. Chem. B, Vol. 111, No. 18, 2007*

Arzhantsev et al.

Figure 8. Time constants of the slower component of the dynamics $S_2(t)$ measured here by combining KGE and TCSPC experiments with t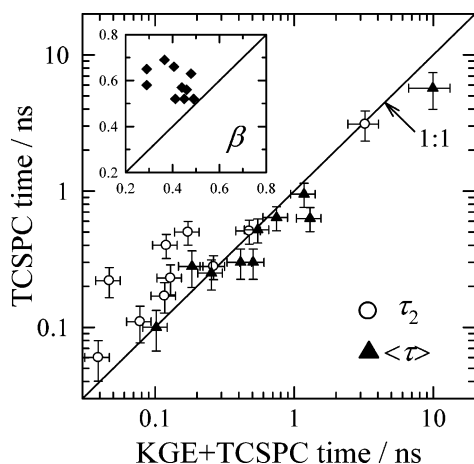he time constants measured using TCSPC alone. τ_2 refers to the time constant, and $\langle\tau\rangle$ the integral time from stretched-exponential fits to the data. The inset shows the stretching exponents β.

both $\nu_{pk}(t)$ curves, so the comparisons made here reflect only the effect of the time resolution on the results. Figure 7 shows that, with the 25 ps response of our system, when $\tau_2 \approx 0.5$ ns, as it is in the case of [Im$_{41}^+$][Tf$_3$C$^-$], TCSPC measurements provide a good representation of the slow component of solvation. Although there are some differences in the values of τ_2 and β derived from the two data sets, the differences are small in this case. However, when the "slow" component is sufficiently fast, as in the case of [Im$_{41}^+$][BF$_4^-$] ($\tau_2 \approx 100$ ps), there is significant distortion of even this slower portion of the response.

The situation is summarized in Figure 8 where we have plotted characteristic times and exponents of all of the comparisons of this sort currently available. For the cases studied here (60 ps $\leq \tau_2 \leq 3$ ns) the exponent β measured with TCSPC alone is higher than that determined from more complete measurements by an average of 0.18 (50%), and the values of τ_2 are an average of 75% larger. Because the effects of these two systematic errors tend to oppose one another, the integral solvation times determined from TCSPC ($\langle\tau\rangle$, filled triangles) are much closer to the correct values than are the τ_2 times. The TCSPC values are systematically smaller, but only by an average of 20%, than those determined from the KGE + TCSPC measurements. On the basis of these observations, it would appear that TCSPC measurements with only 25 ps resolution fortuitously provide reasonably accurate integral solvation times of the slower solvation component, at least for ionic liquids of the sort examined here.

D. Comparisons with Predictions of Dielectric Continuum Models. In conventional dipolar solvents, solvation dynamics is closely linked to the frequency-dependent dielectric response of the solvent, $\epsilon(\omega)$. A number of studies have shown that solvation times[68,77] and even the detailed time dependence of $S_\nu(t)$[68,78–82] can be reproduced with surprising accuracy in dipolar solvents. Several recent reports have suggested that the same might be true in ionic liquids.[19,20,46] Emerging dielectric data from the Weingärtner group[16,83] allow us to test this suggestion in three of the ionic liquids studied here, [Im$_{41}^+$][BF$_4^-$], [Im$_{41}^+$][PF$_6^-$], and [Im$_{41}^+$][Tf$_2$N$^-$].

The solvation model that we adopt is that of a spherical polarizable point dipole solute in a continuum dielectric fluid. The equilibrium solute−solvent interaction energy in such a model can be written[84]

$$E = -\left(\frac{\mu^2}{a^3}\frac{(\epsilon_u + 2)}{3}\right)\frac{(\epsilon - 1)}{(\epsilon + (^1/_2)\epsilon_u)} = -A\hat{\chi}(0) \quad (4)$$

where a is the solute radius, μ its dipole moment, and ϵ_u a cavity dielectric constant representing its polarizability via the relation $(\epsilon_u - 1)/(\epsilon_u + 2) = \alpha a^3$.[84] The normalized response to a step-function change in the solute dipole moment, to be compared to the experimental $S_\nu(t)$ is given by[85,86]

$$S_{\Delta E}(t) = \frac{L_p^{-1}\{(\hat{\chi}(\infty) - \hat{\chi}(p))/p\}}{\hat{\chi}(\infty) - \hat{\chi}(0)} \quad (5)$$

where L_p^{-1} denotes an inverse Laplace transform and

$$\hat{\chi}(p) = \frac{\hat{\epsilon}(p) - 1}{\hat{\epsilon}(p) + (^1/_2)\epsilon_u} \quad (6)$$

with $\hat{\epsilon}(p)$ representing the frequency-dependent dielectric function at frequency $p = i\omega$ and $\hat{\chi}(\infty)$ the susceptibility at frequencies where nuclear solvent motions no longer contribute. For calculating $\hat{\chi}(\infty)$ we take $\hat{\epsilon}(\infty) = n_D^2$ where n_D is the optical index of refraction.

In the Supporting Information we compare predictions of $S_{\Delta E}(t)$ made using this model to solvation response functions $S_\nu(t)$ recently measured with DCS in several conventional dipolar solvents.[71] Also provided there are the parametrizations of the dielectric data[16,83] used as inputs to the ionic liquid calculations displayed below. As discussed in detail in ref 68, experimental $\epsilon(\omega)$ data are seldom available over the entire frequency range required for such calculations, and to perform meaningful comparisons to solvation results some account of the missing components of $\epsilon(\omega)$ is essential. In the present case, the dielectric data cover only microwave frequencies up to 20 GHz,[16] and they therefore do not include the important terahertz region of the spectrum. Although the missing frequency region only accounts for a small fraction of the total dielectric range (that from ϵ_∞^{MW} to n_D^2), contributions from this region have important effects on the calculated dynamics,[68] and they cannot be neglected. In the present context we attempt to account for such missing contributions to $\epsilon(\omega)$ in two different ways.

We first assume that the missing components of $\epsilon(\omega)$ correspond directly to the fast portion of the solvation dynamics observed here. In Figure 9 we therefore compare only the slow portion of solvation $S_2(t)$ to what is calculated based solely on the observed microwave portion of $\epsilon(\omega)$. Like $S_2(t)$, the predictions of such calculations are well represented by stretched-exponential functions of time, and the fit parameters are compiled in Figure 9. These comparisons show that in [Im$_{41}^+$][BF$_4^-$] and [Im$_{41}^+$][Tf$_2$N$^-$] the observed and calculated decays are similar in shape ($\Delta\beta \leq 0.08$), but the calculated decay times τ_2 are faster than those observed by factors of 5−7. In the case of [Im$_{41}^+$][PF$_6^-$] there is better agreement in the time constants, but the shapes (β) differ more significantly. Using the integral solvation times as an overall figure of merit, we find that the calculated response functions are faster than experiment by factors of 5, 11, and 3.5 in the BF$_4^-$, PF$_6^-$, and Tf$_2$N$^-$ liquids, respectively. This level of agreement is rather poor compared to what is usually found in the case of dipolar solvents. (see Supporting Information and refs 68 and 77).

A second comparison, one that we believe is more rigorous, is provided in Figure 10. Here the full solvation response $S_\nu(t)$ is compared to calculations in which we approximate the unobserved portion of $\epsilon(\omega)$ by an additional Debye relaxation function with amplitude $\epsilon_\infty^{MW} - n_D^2$ and a time constant chosen
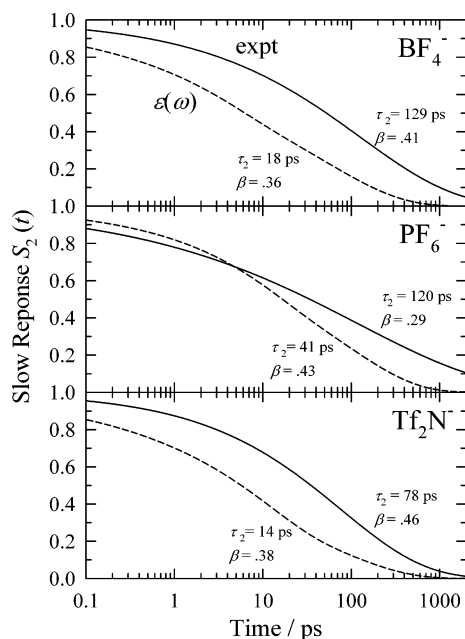
Complete Solvation Response in Ionic Liquids

J. Phys. Chem. B, Vol. 111, No. 18, 2007 **4985**

Figure 9. Comparison of the slow component of the solvation response $S_2(t)$ (solid curves) in several $[Im_{41}^+][X^-]$ liquids to dielectric continuum predictions using only the observed portion of $\epsilon(\omega)$ (dashed curves). The dielectric predictions are well fit by stretched-exponential functions, and the parameters of both the observed and the predicted decays are indicated.
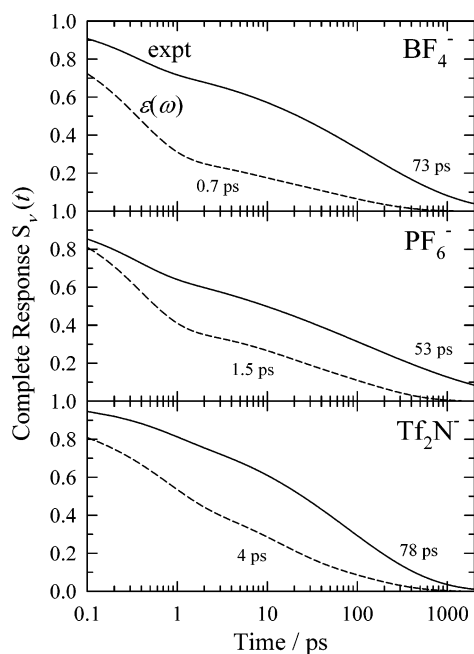

Figure 10. Comparison of the total solvation response $S_\nu(t)$ (solid curves) in several $[Im_{41+}][X^-]$ liquids to dielectric continuum predictions (dashed curves). In these dielectric calculations the portion of $\epsilon(\omega)$ missing from the microwave experiments has been approximated by an additional Debye process with a longitudinal relaxation time equal to the experimental value of τ_1 (see text). Times indicated are the $1/e$ times of the decays.

to match the experimental value of τ_1. Approximation of missing of $\epsilon(\omega)$ components in this manner leads to even worse agreement between the predictions and the experimental data. The amplitudes of the fast component are exaggerated in the calculated decays, and their inclusion makes the calculated times, which were already too small, even smaller. Quantitatively, we

find the predicted $1/e$ times of the response to be factors of 100, 35, and 19 smaller than the corresponding experimental times.

On the basis of the above comparisons we conclude that the same relationships between $\epsilon(\omega)$ and $S_\nu(t)$ of proven utility for predicting solvation response functions in dipolar solvents are not applicable to ionic liquids. This observation is not surprising given the fact that the solvation energies of dipolar solutes do not bear the same relationship to the static dielectric constants of ionic liquids as do solvation energies in dipolar liquids. For example, ϵ in the ionic liquids studied here ranges between 10.4 and 11.5 whereas the Stokes shifts of DCS in these solvents are larger than those in dipolar liquids such as dimethylsulfoxide ($\epsilon = 46$). Clearly the dynamics underlying $\epsilon(\omega)$ and $S_\nu(t)$ have much in common, and it might be possible to derive accurate approximate connections between the two. But the present results indicate that this connection must differ in important ways from that pertaining in dipolar liquids.

E. Comparisons to Simulation. We now compare the present results with available computer simulations of solvation dynamics and consider the nature of the molecular motions responsible for the observed dynamics. A number of simulations of time-dependent solvation have been performed using realistic models of imidazolium ionic liquids.[53−61] The computational expense of such simulations has thus far prohibited adequate simulation of the slow, nanosecond portion of the response, and for this reason we confine comparisons to the short-time, sub-picosecond portion. Simulation results concerning the amplitude f_1 and time constant τ_1 of the initial response are collected in Table 3. Data here are grouped primarily in terms of the solute and then secondarily by the solvent studied.

The first simulations of solvation dynamics in ionic liquids were performed by Kim and co-workers[53] who examined solvation of a diatomic model solute undergoing a transition between a nonpolar state and an ion-pair state in which the atoms are charged to $\pm 1e$. In models of $[Im_{21}^+][Cl^-]$ and $[Im_{21}^+][PF_6^-]$ solvents at 400 K, they observed markedly biphasic response functions wherein over half of the solvation energy relaxed via sub-picosecond Gaussian components while the remainder relaxed in nonexponential decays that were too slow to be adequately sampled.[53,55] The fast Gaussian response was attributed to inertial translations of ions whereas the slower dynamics were attributed to diffusive transport.[55] Several other workers have subsequently simulated this same diatomic solute in similar ionic-liquid solvents (again at elevated temperatures) and have reported comparable results,[59,61] as listed in Table 3.

Kim and co-workers also simulated a fictitious $\pm 1e$ transition in a model benzene solute and observed qualitatively similar behavior to that of the diatomic solute.[55] However, they found that the amplitude of the initial fast decay is reduced and that the time is increased slightly relative to what was observed in the diatomic solute. Finally, Kobrak and co-workers simulated two realistic models of experimental solutes in $[Im_{41}^+][PF_6^-]$ at 300 K.[56−58] The solutes, solvent, and temperature of these last simulations provide a much closer match to the present experiments than the other simulations just mentioned. What Kobrak found was that although the time constants associated with the initial Gaussian component are comparable to those in the other simulations, the amplitudes of the fast components are greatly reduced. Kobrak also reported that solute motion and rotation of the Im_{41}^+ cation play negligible roles in the fast initial response, and he emphasized the highly coupled nature of cation and anion motions.[58]

TABLE 3: Summary of Simulated Fast Response Characteristics[a]

solute	perturbation	$\Delta\mu$ (D)	simulation type	ionic liquid	T (K)	f_1	τ_1 (ps)	reference
diatomic[b]	$00 \to \pm 1e$	19.2	eq. IP	$[Im_{11}^+][Cl^-]$	425	0.76	0.069	61
			n.e.	$[Im_{21}^+][Cl^-]$	400	0.75	0.14	55
			n.e.	$[Im_{21}^+][PF_6^-]$	400	0.63	0.21	55
			n.e.	$[Im_{61}^+][PF_6^-]$	378	<0.7	0.27	59
benzene	"natural" $\to \pm 1e$ para C	13.5	n.e.	$[Im_{21}^+][Cl^-]$	400	0.65	0.13	55
			n.e.	$[Im_{21}^+][PF_6^-]$	400	0.69	0.18	55
betaine-30	S_1-S_0 distribution	-14.6	eq. S_0	$[Im_{41}^+][PF_6^-]$	300	0.31	0.17	57
coumarin 153	S_1-S_0 distribution	7.7	eq. S_0	$[Im_{41}^+][PF_6^-]$	300	0.12	0.21	58
DCS	S_1-S_0 distribution	$10-15^c$	expt	$[Im_{n1}^+][X^-]$	298	$0.1-0.2$	$0.1-0.7$	this work
			expt	$[Im_{41}^+][PF_6^-]$	298	$0.19 \pm .03$	$0.33 \pm .08$	this work

[a] "Perturbation" describes the charge perturbation applied in the case of nonequilibrium simulations (simulation type = "n.e.") and to the charge differences from which S_1-S_0 energy differences ΔE are calculated in the case of equilibrium simulations. In the latter case, simulation type = "eq. IP" and "eq. S_0" indicate that the solvation response is estimated from equilibrium time correlation functions of ΔE calculated in the presence of the ion pair ($\pm 1e$) and S_0 charge distributions, respectively. $\Delta\mu$ is the difference in solute dipole moment resulting from the perturbation. In all cases the simulations find the initial solvation component to have a clearly Gaussian character. To compare the simulation results to our experimental data, which employ an exponential fit of this component, we refit the simulation data to either the functional form in eq 2 or converted reported Gaussian time constants τ_g (from $\exp(-t^2/\tau_g^2)$) via $\tau_1 \cong 0.90\tau_g$. [b] Diatomic refers to a solute that has a bond length of 3.5 Å and Lennard-Jones parameters $\sigma = 4$ Å and $\epsilon/k_B = 100$ K. [c] Estimated from the solvatochromic analysis in ref 71.

Comparing these simulations results with our measured values (the last two rows of Table 3), we conclude that there is general agreement with respect to the extent and time scale of the initial solvation response. The variations in the dynamics simulated with different solutes suggest that the amplitude of the initial response is small and comparable to what is observed here when the solute perturbation does not involve large and/or highly localized charges. The fact that the experimental value of f_1 observed for DCS in $[Im_{41}^+][PF_6^-]$ lies between the values simulated for the $S_0 \to S_1$ transitions of C153 and betaine-30 in this solvent is consistent with what might be expected based on the nature of the transitions in these three molecules. Although there is significant uncertainty in the measured values of τ_1 and we do not have the time resolution to actually observe the Gaussian character of the early response, it appears that the experimental times are somewhat larger than those predicted by simulation. This difference might be due to the neglect of electronic polarizability in the simulations, which would be expected to slow the simulated response.[87,88] Finally, although there are few simulation data, the trends observed upon varying the anion size or mass are at least qualitatively similar in experiment and simulation.

F. Solvation "Mechanism". Given the correspondence described in the last section and the insights gleaned from simulation, we conclude by asking what can now be said of the molecular "mechanism" of the solvation response in ionic liquids. First, we note that both simulation and experiment argue against our earlier suggestion[33] that imidazolium cations might be specifically responsible for producing the fast component of the response. This idea was based on the absence of unresolvable fast components in the few non-imidazole ionic liquids that we had measured at the time.[33] But comparison of the present data on $[Pr_{31}^+][Tf_2N^-]$ and $[Im_{41}^+][Tf_2N^-]$ as well as TCSPC data on a number of other pyrrolidinium and ammonium ionic liquids[31,89] shows that an imidazolium cation is not necessary or sufficient to produce a fast initial response. If anything, emerging simulation data point to the anion (or more likely the smallest ion present) as primarily dictating the time scale of the fastest response.

It is clear that the fastest portions of solvation result from inertial ion motions. These dynamics are presumably the translational equivalent of the "free-streaming" rotational motion that gives rise to the initial Gaussian component in conventional dipolar solvents.[21] In small and highly polar solvents such as

acetonitrile,[90] this initial Gaussian contribution accounts for well over half of the solvation response. The first simulations on ionic liquids[53,55] and the early experimental observations of large unresolved components in ionic liquids[32] seemed to point to a similarly pronounced inertial component in ionic liquids. But the present experiments and Kobrak's simulations of solvatochromic solutes[57,58] suggest instead that the amplitude of the sub-picosecond, inertial component will typically be much smaller, probably 20% or less. As discussed in section 3C, it now seems likely that in the many cases where ~50% of the expected Stokes shift was missed in TCSPC and other experiments[31-33,35,44] the majority of the missing dynamics should actually be attributed the fastest portions of the broadly distributed "slow" dynamics rather than being associated with sub-picosecond inertial dynamics. We also note that the inertial component in $[Im_{41}^+][PF_6^-]$ and other ionic liquids is entirely absent at temperatures near the liquid's glass transition.[19,20] This freezing is probably due to the reduction in free volume available for ion motion with decreasing temperature, as suggested in earlier temperature-dependent measurements.[33] Thus, we conclude that the initial Gaussian component of solvation dynamics will generally have a much more modest effect in ionic liquids in comparison to highly polar conventional solvents.

The majority of the solvation response appears to result from a single continuous process, which can be represented by a stretched-exponential relaxation with values of β in the range of $0.3-0.5$. The fact that the times associated with this component are correlated with solvent viscosity (Figure 6) implies that the underlying motions are coupled to structural reorganization of the liquid. Useful perspective on this phase of solvation as well as the free-streaming phase can be obtained by considering the extent of ion motion possible during the observed solvation times. For simplicity, we focus on translational motions of ions and estimate the translational displacement resulting from free-streaming dynamics via

$$\Delta r_i^{free}(t) \cong v_i^{rms} t = \sqrt{\frac{3k_B T}{M_i}}\, t \tag{7}$$

and from ion diffusion using

$$\Delta r_i^{diff}(t) \cong \sqrt{6 D_i t} \tag{8}$$

Complete Solvation Response in Ionic Liquids

J. Phys. Chem. B, Vol. 111, No. 18, 2007 **4987**

TABLE 4: Estimates of Ion Translation during Solvation[a]

ionic liquid	τ_1 (ps)	$(\Delta r_+^{\text{free}}(\tau_1))/2R_+$	$(\Delta r_-^{\text{free}}(\tau_1))/2R_-$	D_+ (10^{12} m^2 s^{-1})	D_- (10^{12} m^2 s^{-1})	$t_{0.1}$ (ns)	$(\Delta r_+^{\text{diff}}(t_{0.1}))/2R_+$	$(\Delta r_-^{\text{diff}}(t_{0.1}))/2R_-$
[Im$_{61}^+$][Cl$^-$]	0.10	0.03	0.11					
[Im$_{41}^+$][BF$_4^-$]	0.32	0.11	0.21	14.5	10.2	0.79	0.39	0.48
[Im$_{41}^+$][PF$_6^-$]	0.33	0.11	0.15	7.1	3.8	1.54	0.38	0.38
[Im$_{41}^+$][Tf$_2$N$^-$]	0.74	0.25	0.19	27.5	17.4	0.45	0.40	0.33

[a] τ_1 is the time constant of the initial solvation response (eq 2), and $\Delta r_i^{\text{free}}(\tau_1)$ is the free displacement of an ion of type i (+ or −) during this time according to eq 7. D_i is the experimental diffusion constant of species i calculated from the parametrizations in Tokuda et al.[100] $t_{0.1}$ is the time required for $S_v(t)$ to reach a value of 0.10, and $\Delta r_i^{\text{diff}}(t_{0.1})$ is the diffusive displacement of an ion i during this time, calculated using eq 8. Displacements are shown in terms of ion diameters $2R_i$ (with the R_i from Table 1).

In Table 4 we provide estimates of (i) the average ion displacement caused by free-streaming motion during the initial time τ_1 using eq 7 and (ii) the average displacement resulting from diffusive motion during the total time required for $S_v(t)$ to decay to 10%, $t_{0.1}$. What these calculations show is that the initial phase of solvation characterized by τ_1 is sufficiently short that ions only have time to move a small distance (<1 Å), approximately 10−20% of their diameters. This observation is not surprising. If the observed sub-picosecond response is largely free-streaming motion of ions, then the available free volume around ions or the solute should limit the average range of such motions to small fractions of the ion sizes. Much more surprising is the fact that, as estimated via eq 8, diffusive motions of ions also entail only modest displacements by the time that 90% of the solvation is complete. As indicated in Table 4, by the time $S_v(t) = 0.1$, ions have translated on average only approximately 40% of their diameters. Although this calculation is crude and neglects both modification of ion motions by the presence of the solute and contributions from rotational motions, simulations on model ionic liquids currently in progress[91] suggest that the basic idea is correct. Solvation is largely accomplished before ions have, on average, traveled distances required for exchange of their coordination spheres.

On the basis of the above observations and motivated by prior work on solvation in dipolar liquids,[21] we tentatively propose the following description of solvation dynamics in ionic liquids. Immediately after solute excitation, ions move largely independently of one another in response to the solute. They move independently but from a set of initial conditions in which ion coordinates are very strongly correlated.[21,92] This phase of the motion, which accounts for a minor fraction of the total response, lasts for less than a picosecond, after which time ions collide with the cage formed by their immediate neighbors. The bulk of the solvation takes place during a period in which most ions remain confined by the cage of neighbors that initially surround them at time zero. Computer simulations show that translation[93−95] and rotation[95,96] in ionic liquids entail long episodes of rattling and librational motions within such cages, a feature characteristic of glassy dynamics. Solvation is likely to be associated with cage deformation and reformation processes that occur during and as a result of such caged motions. The fact that cage deformation/reformation processes would be expected to depend on solvent viscosity and be governed by a broad distribution of times is consistent with the observed viscosity dependence and stretched-exponential character of the primary solvation response. Finally, we note that it is to be expected that only small distortions of the original solvation structure should be required to effect solvation in ionic liquids for the same reason that very little motion is required in the case of highly polar conventional solvents.[21,97] The strong coupling among ions in an ionic liquid renders solvation a highly collective process such that the energetic perturbation brought about by a solute transition can be easily relaxed by only minor adjustments of the positions and possibly orientations of nearby ions.

4. Conclusions

We have presented KGE + TCSPC measurements of the complete solvation response in six ionic liquids using the probe DCS. Comparisons between TCSPC results on DCS and the more popular probe C153 suggest that the dynamics measured here should be directly comparable to results measured using other polar solvation probes. Solvation in the imidazolium and pyrrolidinium liquids studied here is biphasic, consisting of a minor (10−20%) sub-picosecond component associated with inertial solvent motions and a broadly distributed "slow" component coupled to structural reorganization in the solvent. The KGE measurements indicate that substantial portions of even the slower component of the solvation response are missed in experiments such as TCSPC with response times of 25 ps or larger. However, in many cases a fortuitous cancellation of errors renders estimates of the integral slow times from such experiments of reasonable accuracy. As one means for interpreting the observed dynamics, we compared the solvation response measured in three ionic liquids for which dielectric data were available to predictions of the dielectric continuum models. These comparisons showed that the same models previously found quite successful for predicting solvation times in dipolar solvents yield highly inaccurate predictions in the case of ionic liquids. Finally, by combining insights from simulation studies and simple considerations of the extent of ion motion, we proposed a tentative description of the nature of the ion motions responsible for solvation in ionic liquids. Further simulation work should help to refine this description.

References and Notes

(1) *Ionic Liquids in Synthesis*; Wasserscheid, P.; Welton, T., Eds.; Wiley-VCH: Weinheim, Germany, 2003.

(2) Chiappe, C.; Pieraccini, D. *J. Phys. Org. Chem.* **2005**, *18*, 275−297.

(3) Poole, C. F. *J. Chromatogr., A.* **2004**, *1037*, 49−82.

(4) Reichardt, C. *Green Chem.* **2005**, *7*, 339−351.

(5) Abraham, M.; Acree, W. E. *Green Chem.* **2006**, *8*, 906−915.

(6) Hyun, B. R.; Dzyuba, S. V.; Bartsch, R. A.; Quitevis, E. L. *J. Phys. Chem. A* **2002**, *106*, 7579−7585.

(7) Rajian, J. R.; Li, S.; Bartsch, R. A.; Quitevis, E. L. *Chem. Phys. Lett.* **2004**, *393*, 372−377.

(8) Xiao, D.; Rajian, J. R.; Li, S.; Bartsch, R. A.; Quitevis, E. L. *J. Phys. Chem. B* **2006**, *110*, 16174−16178.

(9) Giraud, G.; Gordon, C. M.; Dunkin, I. R.; Wynne, K. *J. Chem. Phys.* **2003**, *119*, 464−477.

(10) Cang, H.; Li, J.; Fayer, M. D. *J. Chem. Phys.* **2003**, *119*, 13017−13023.

(11) Li, J.; Wang, I.; Fruchey, K.; Fayer, M. D. *J. Phys. Chem. A* **2006**, *110*, 10384−10391.

(12) Shirota, H.; Castner, E. W., Jr. *J. Phys. Chem. A* **2005**, *109*, 9388−9392.

(13) Shirota, H.; Funston, A. M.; Wishart, J. F.; Castner, E. W., Jr. *J. Chem. Phys.* **2005**, *122*, 184512.

(14) Ribeiro, M. C. C. *J. Phys. Chem. B* **2007**, *111*, 5008−5015.

(15) Weingärtner, H.; Knocks, A.; Schrader, W.; Kaatze, U. *J. Phys. Chem.* **2001**, *105*, 8646−8650.

(16) Daguenet, C.; Dyson, P. J.; Krossing, I.; Oleinikova, A.; Slattery, J.; Wakai, C.; Weingärtner, H. *J. Phys. Chem. B* **2006**, *110*, 12682−12688.

(17) Rivera, A.; Rossler, E. A. *Phys. Rev. B* **2006**, *73*, 212201.

(18) Schroedle, S.; Annat, G.; MacFarlane, D. R.; Forsyth, M.; Buchner, R.; Hefter, G. *Chem. Commun.* **2006**, 1748−1750.

(19) Ito, N.; Huang, W.; Richert, R. *J. Phys. Chem. B* **2006**, *110*, 4371−4377.

(20) Ito, N.; Richert, R. *J. Phys. Chem. B* **2007**, *111*, 5016−5022.

(21) Stratt, R. M.; Maroncelli, M. *J. Phys. Chem.* **1996**, *100*, 12981−12996.

(22) Bart, E.; Huppert, D. *Chem. Phys. Lett.* **1992**, *195*, 37−44.

(23) Bart, E.; Meltsin, A.; Huppert, D. *Chem. Phys. Lett.* **1992**, *200*, 592−596.

(24) Bart, E.; Meltsin, A.; Huppert, D. *J. Phys. Chem.* **1994**, *98*, 3295−3299.

(25) Bart, E.; Meltsin, A.; Huppert, D. *J. Phys. Chem.* **1994**, *98*, 10819−10823.

(26) Karmakar, R.; Samanta, A. *J. Phys. Chem. A* **2002**, *106*, 4447−4452.

(27) Karmakar, R.; Samanta, A. *J. Phys. Chem. A* **2002**, *106*, 6670−6675.

(28) Karmakar, R.; Samanta, A. *J. Phys. Chem. A* **2003**, *107*, 7340−7346.

(29) Saha, S.; Mandal, P. K.; Samanta, A. *Phys. Chem. Chem. Phys.* **2004**, *6*, 3106−3110.

(30) Mandal, P. K.; Paul, A.; Samanta, A. *Res. Chem. Intermed.* **2005**, *31*, 575−583.

(31) Mandal, P. K.; Samanta, A. *J. Phys. Chem. B* **2005**, *109*, 15172−15177.

(32) Ingram, J. A.; Moog, R. S.; Ito, N.; Biswas, R.; Maroncelli, M. *J. Phys. Chem. B* **2003**, *107*, 5926−5932.

(33) Arzhantsev, S.; Ito, N.; Heitz, M.; Maroncelli, M. *Chem. Phys. Lett.* **2003**, *381*, 278−286.

(34) Ito, N.; Arzhantsev, S.; Heitz, M.; Maroncelli, M. *J. Phys. Chem. B* **2004**, *108*, 5771−5777.

(35) Ito, N.; Arzhantsev, S.; Maroncelli, M. *Chem. Phys. Lett.* **2004**, *396*, 83−91.

(36) Arzhantsev, S.; Jin, H.; Baker, G. A.; Ito, N.; Maroncelli, M. In *Femtochemistry VII: Fundamental Ultrafast Processes in Chemistry, Physics, and Biology*; Castleman, A. W., Kimble, M. L., Eds., Elsevier: Amsterdam, 2006.

(37) Arzhantsev, S.; Jin, H.; Ito, N.; Maroncelli, M. *Chem. Phys. Lett.* **2006**, *417*, 524−529.

(38) Chakrabarty, D.; Hazra, P.; Chakraborty, A.; Seth, D.; Sarkar, N. *Chem. Phys. Lett.* **2003**, *381*, 697−704.

(39) Chakrabarty, D.; Chakraborty, A.; Seth, D.; Hazra, P.; Sarkar, N. *Chem. Phys. Lett.* **2004**, *397*, 460−474.

(40) Chakrabarty, D.; Chakraborty, A.; Seth, D.; Sarkar, N. *J. Phys. Chem. A* **2005**, *109*, 1764−1769.

(41) Chakrabarty, D.; Seth, D.; Chakraborty, A.; Sarkar, N. *J. Phys. Chem. B* **2005**, *109*, 5753−5758.

(42) Chakraborty, A.; Seth, D.; Chakrabarty, D.; Setua, P.; Sarkar, N. *J. Phys. Chem. A* **2005**, *109*, 11110−11116.

(43) Chowdhury, P. K.; Halder, M.; Sanders, L.; Calhoun, T.; Anderson, J. L.; Armstrong, D. W.; Song, X.; Petrich, J. W. *J. Phys. Chem. B* **2004**, *108*, 10245−10255.

(44) Sanders, Headley, L.; Mukherjee, P.; Anderson, J. L.; Ding, R.; Halder, M.; Armstrong, D. W.; Song, X.; Petrich, J. W. *J. Phys. Chem. A* **2006**, *110*, 9549−9554.

(45) Mukherjee, P.; Crank, J. A.; Halder, M.; Armstrong, D. W.; Petrich, J. W. *J. Phys. Chem. A* **2006**, *110*, 10725−10730.

(46) Halder, M.; Headley, L. S.; Mukherjee, P.; Song, X.; Petrich, J. W. *J. Phys. Chem. A* **2006**, *110*, 8623−8626.

(47) Baker, S. N.; Baker, G. A.; Munson, C. A.; C., F.; Bukowski, E. J.; Cartwright, A. N.; Bright, F. V. *Ind. Eng. Chem. Res.* **2003**, *42*, 6457−6463.

(48) Wishart, J. F.; Lall-Ramnarine, S. I.; Raju, R.; Scumpia, A.; Bellevue, S.; Ragbir, R.; Engel, R. *Radiat. Phys. Chem.* **2005**, *72*, 99−104.

(49) Lang, B.; Angulo, G.; Vauthey, E. *J. Phys. Chem. A* **2006**, *110*, 7028−7034.

(50) Mandal, P. K.; Saha, S.; Karmakar, R.; Samanta, A. *Curr. Sci.* **2006**, *90*, 301−310.

(51) Samanta, A. *J. Phys. Chem. B* **2006**, *110*, 13704−13716.

(52) Fee, R. S.; Maroncelli, M. *Chem. Phys.* **1994**, *183*, 235−247.

(53) Shim, Y.; Duan, J.; Choi, M. Y.; Kim, H. J. *J. Chem. Phys.* **2003**, *119*, 6411−6414.

(54) Shim, Y.; Choi, M. Y.; Kim, H. J. *J. Chem. Phys.* **2005**, *122*, 044510.

(55) Shim, Y.; Choi, M. Y.; Kim, H. J. *J. Chem. Phys.* **2005**, *122*, 044511.

(56) Znamenskiy, V.; Kobrak, M. N. *J. Phys. Chem. B* **2004**, *108*, 1072−1079.

(57) Kobrak, M. N.; Znamenskiy, V. *Chem. Phys. Lett.* **2004**, *395*, 127−132.

(58) Kobrak, M. N. *J. Chem. Phys.* **2006**, *125*, 064502.

(59) Margulis, C. J. *Mol. Phys.* **2004**, *102*, 829−838.

(60) Hu, Z.; Margulis, C. J. *J. Phys. Chem. B* **2006**, *110*, 11025−11028.

(61) Bhargava, B. L.; Balasubramanian, S. *J. Chem. Phys.* **2005**, *123*, 144505.

(62) Gardecki, J. A.; Maroncelli, M. *J. Phys. Chem. A* **1999**, *103*, 1187−1197.

(63) Arzhantsev, S.; Maroncelli, M. *Appl. Spectrosc.* **2005**, *59*, 206−220.

(64) Baker, S. N.; McCleskey, T. M.; Pandey, S.; Baker, G. A. *Chem. Commun.* **2004**, 940−941.

(65) Nockemann, P. B., K.; Driesen, K. *Chem. Phys. Lett.* **2005**, *415*, 131.

(66) Baker, G. A., to be submitted for publication.

(67) Heitz, M. P.; Maroncelli, M. *J. Phys. Chem. A* **1997**, *101*, 5852−5868.

(68) Horng, M. L.; Gardecki, J. A.; Papazyan, A.; Maroncelli, M. *J. Phys. Chem.* **1995**, *99*, 17311−17337.

(69) Gardecki, J. A.; Maroncelli, M. *Appl. Spectrosc.* **1998**, *52*, 1179−1189.

(70) Il'ichev, Y. V.; Kuehnle, W.; Zachariasse, K. A. *Chem. Phys.* **1996**, *211*, 441−453.

(71) Arzhantsev, S.; Zachariasse, K.; Maroncelli, M. *J. Phys. Chem. B* **2006**, *110*, 3454−3470.

(72) El-Gezawy, H.; Rettig, W. *Chem. Phys.* **2006**, *327*, 385−394.

(73) Görner, H.; Kuhn, H. J. *Adv. Photochem.* **1995**, *19*, 1−117.

(74) Il'ichev, Y. V.; Zachariasse, K. A. *Ber. Bunsen Phys. Chem.* **1997**, *101*, 625−635.

(75) Strictly speaking, the initial response should be Gaussian in character so that $(dv(t)/dt)_{t=0} = 0$; however, our time resolution does not allow us to distinguish between Gaussian and exponential representations, and we use the exponential form for convenience.

(76) Ashcroft, N. W.; Mermin, N. D. *Solid State Physics*; Saunders College Publishing: Philadelphia, PA, 1976.

(77) Maroncelli, M. *J. Chem. Phys.* **1997**, *106*, 1545−1555.

(78) Hsu, C. P.; Song, X.; Marcus, R. A. *J. Phys. Chem. B* **1997**, *101*, 2546−2551.

(79) Hsu, C. P.; Georgievskee, Y.; Marcus, R. A. *J. Phys. Chem. A* **1998**, *102*, 2658−2666.

(80) Song, X.; Chandler, D. *J. Chem. Phys.* **1998**, *108*, 2594−2600.

(81) Lustres, J. L. P.; Kovalenko, S. A.; Mosquera, M.; Senyushkina, T.; Flasche, W.; Ernsting, N. P. *Angew. Chem., Int. Ed.* **2005**, *44*, 5635−5639.

(82) Ruthmann, J.; Kovalenko, S. A.; Ernsting, N. P.; Ouw, D. *J. Chem. Phys.* **1998**, *109*, 5466−5468.

(83) Weingärtner, H. Unpublished results, 2006.

(84) Böttcher, C. J. F.; van Belle, O. C.; Bordewijk, P.; Rip, A. *Theory of Electric Polarization: Dielectrics in Static Fields*, 2nd ed.; Elsevier: Amsterdam, 1973; Vol. I.

(85) Wolynes, P. G. *J. Chem. Phys.* **1987**, *86*, 5133−5136.

(86) Rips, I.; Klafter, J.; Jortner, J. *J. Chem. Phys.* **1988**, *88*, 3246−3252.

(87) Bursulaya, B.; Zichi, D. A.; Kim, H. J. *J. Phys. Chem.* **1995**, *99*, 10069−10074.

(88) Kumar, P. V.; Maroncelli, M. *J. Chem. Phys.* **1995**, *103*, 3038−3060.

(89) Jin, H.; Baker, G. A.; Arzhantsev, S.; Dong, J.; Maroncelli, M. Solvation and Rotational Dynamics of Coumarin 153 in Ionic Liquids−Comparisons to Conventional Solvents. *J. Phys. Chem. B*, submitted for publication.

(90) Maroncelli, M. *J. Chem. Phys.* **1991**, *94*, 2084−2103.

(91) Maroncelli, M.; Conte, S. Unpublished results.

Complete Solvation Response in Ionic Liquids

J. Phys. Chem. B, Vol. 111, No. 18, 2007 **4989**

(92) Ladanyi, B. M.; Maroncelli, M. *J. Chem. Phys.* **1998**, *109*, 3204−3221.

(93) Margulis, C. J.; Stern, H. A.; Berne, B. J. *J. Phys. Chem. B* **2002**, *106*, 12017−12021.

(94) Del Popolo, M. G.; Voth, G. *J. Phys. Chem. B* **2004**, *108*, 1744−1752.

(95) Hu, Z.; Margulis, C. J. *Proc. Natl. Acad. Sci. U.S.A.* **2006**, *103*, 831−836.

(96) Shim, Y.; Jeong, D.; Choi, M. Y.; Kim, H. J. *J. Chem. Phys.* **2006**, *125*, 061102.

(97) Maroncelli, M.; Kumar, V. P.; Papazyan, A. *J. Phys. Chem.* **1993**, *97*, 13−17.

(98) Jin, H.; O'Hare, B.; Dong, J.; Arzhantsev, S.; Baker, G. A.; Wishart, J. F.; Benesi, A.; Maroncelli, M. Physical Properties of Ionic Liquids Consisting of the Bis(trifluoromethylsulfonyl)imide Anion with Various Cations and the 1-Butyl-3-Methyl Imidazolium Cation with Various Anions. *J. Phys. Chem. B*, to be submitted for publication**.**

(99) Bondi, A. *J. Phys. Chem.* **1964**, *68*, 441−451.

(100) Tokuda, H.; Kikuko, H.; Ishii, K.; Susan, M. A. B. H.; Watanabe, M. *J. Phys. Chem. B* **2004**, *108*, 16593−16600.